

# Avalanche-driven fractal flux distributions in NbN superconducting films

I. A. Rudnev

Moscow Engineering Physics Institute, 115409 Moscow, Russia

D. V. Shantsev

Department of Physics, University of Oslo, P. O. Box 1048 Blindern, 0316 Oslo, Norway  
and A. F. Ioffe Physico-Technical Institute, Polytekhnicheskaya 26, St. Petersburg 194021, Russia

T. H. Johansen<sup>a)</sup>

Department of Physics, University of Oslo, P. O. Box 1048 Blindern, 0316 Oslo, Norway and Texas Center for Superconductivity and Advanced Materials, University of Houston, Houston, Texas 77204

A. E. Primenko

Department of Low Temperature Physics and Superconductivity, Moscow State University, 117234 Russia

(Received 24 November 2004; accepted 27 May 2005; published online 18 July 2005)

Flux distributions in thin superconducting NbN films placed in a perpendicular magnetic field have been studied using magneto-optical imaging. Below 5.5 K the flux penetrates in the form of abrupt avalanches resulting in dendritic structures. Magnetization curves in this regime exhibit extremely noisy behavior. Stability is restored both above a threshold temperature  $T^*$  and applied field  $H^*$ , where  $H^*$  is smaller for increasing field than during descent. The dendrite size and morphology are strongly  $T$  dependent, and fractal analysis of the first dendrites entering into a virgin film shows that dendrites formed at higher  $T$  have larger fractal dimension. © 2005 American Institute of Physics. [DOI: 10.1063/1.1992673]

Flux jumps are known to destroy the critical state of type-II superconductors and suppress the apparent critical current density.<sup>1,2</sup> In thin films, the flux jumps manifest themselves in a so-called dendritic instability; that is, avalanche-like penetration of magnetic flux along narrow branching channels. Using magneto-optical (MO) imaging the dendritic instability has been observed in superconducting films of Nb,<sup>3-5</sup> YBa<sub>2</sub>Cu<sub>3</sub>O<sub>7- $\delta$</sub>  (triggered by a laser pulse),<sup>6,7</sup> MgB<sub>2</sub>,<sup>8-12</sup> and YNi<sub>2</sub>B<sub>2</sub>C.<sup>13</sup> Recently, flux dendrites were found also in films of Nb<sub>3</sub>Sn,<sup>14</sup> a superconductor with A15 structure widely used in applications.

In the present letter, we report experiments made on niobium nitride (NbN) films, another binary alloy shown here to have dendritic flux penetration in the superconducting state. By combining MO imaging and magnetometry we find threshold values for temperature and applied field above which the dendritic instability disappears. We also analyze striking changes in the size and morphology of the dendrites close to the threshold.

Thin films of NbN were fabricated by magnetron sputtering on sapphire substrates. Two long strips with thickness 0.16 and 0.29  $\mu\text{m}$  width 3 mm and length 10 mm were selected for the present studies. Table I shows their critical temperatures  $T_c$ , the width of the superconducting transition  $\Delta T_c$ , the critical current density  $j_c$  at 4.2 K, and the resistivity  $\rho_N$  in the normal state. All these parameters were obtained from transport measurements using a four-probe method.

The magnetic moment was measured using a PARC vibrating sample magnetometer (EG&G) with a He flow cryostat. Shown in Fig. 1 are magnetization curves  $m(H)$  for the NbN films obtained at 4.2 K. The instability manifests itself here in numerous and random jumps of  $m$ . The jump amplitude varies from  $0.3 \times 10^{-3}$  to  $10^{-3}$  emu. It is much larger

than the sensitivity of the magnetometer,  $3 \times 10^{-5}$  emu, which is represented by the thickness of  $m(H)$  curves in Fig. 1. Magnification of a part of the  $m(H)$  curve (see the inset) shows that the abrupt drops in magnetic moment are followed by a much slower increase before the next drop occurs.

In the thinner film (lower panel) the jumps are seen to disappear above a threshold field  $H^* \approx 1$  kOe on the increasing field branch. Moreover, just below  $H^*$  the jumps in  $m$  have a larger amplitude and occur less frequently than at low fields. On the descending field branch, the jumps reappear when  $m$  is fully reversed, and their amplitude decreases rapidly.

The nature of these jumps in the magnetic moment was clarified using MO imaging to visualize the dynamics of the full flux distribution.<sup>15</sup> The sample, with a Faraday active indicator film placed directly on top, was glued onto the cold finger of an optical cryostat, where it was cooled to 3.5–8 K in zero magnetic field (ZFC). Subsequently, a perpendicular field was applied with the ramp rate 0.5 Oe/s.

For low fields, most of the superconductor is in the Meissner state and appears dark on the MO images. As the field increases, the flux penetrates gradually, starting preferentially from the weak places along the edges. At some field  $H_{ij} \approx 10$  Oe an abrupt invasion of a relatively large flux structure occurred (see Fig. 2). Further field increase resulted in formation of even larger and highly dendritic structures entering one by one. Eventually, when reaching  $H \approx 28$  Oe, the flux dendrites filled most of the film area. Upon further

TABLE I. Parameters of NbN films.

$d$ ( $\mu\text{m}$ )	$T_c$ (K)	$\Delta T_c$ (K)	$j_c$ (MA/cm <sup>2</sup> )	$\rho_N$ ( $\mu\Omega$ m)
0.16	14.2	0.5	1.0	1.6
0.29	15.0	0.5	1.4	1.1

<sup>a)</sup>Electronic mail: t.h.johansen@fys.uio.no

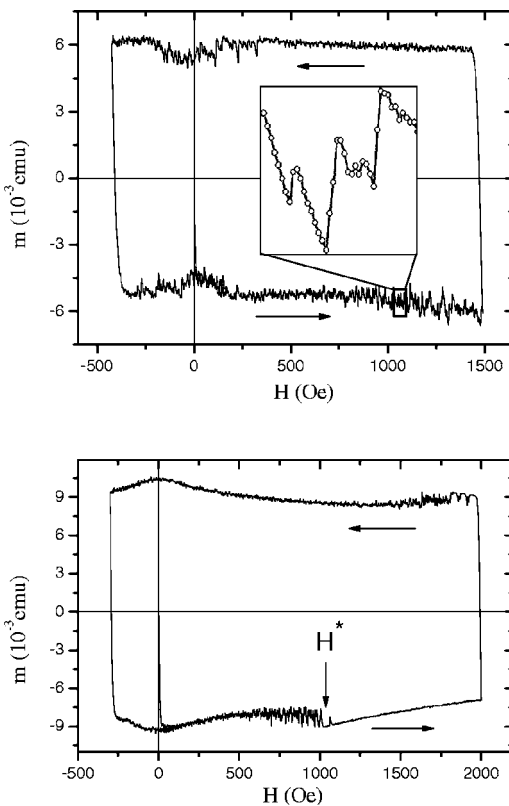


FIG. 1. Magnetic moment as a function of applied field at 4.2 K for two NbN films: 0.29  $\mu\text{m}$  thick (upper) and 0.16  $\mu\text{m}$  thick (lower).

field increase, new dendrites continued to form, but now entering on top of already existing ones, as seen in the MO image taken at 100 Oe. Note that the tilted lines of flux penetration near the edge is of a different origin, most likely due to polishing streaks in the substrate.

Most features of the observed dendritic instability in the NbN films resemble those found previously in other materials.<sup>3-14</sup> The dendrites propagate into the film faster than 1 ms, which is the time resolution of the CCD camera recording our MO images. In fact, we expect that the propagation is even much faster, as was found using ultrafast MO imaging of dendrites in  $\text{YBa}_2\text{Cu}_3\text{O}_{7-\delta}$  and  $\text{MgB}_2$  films.<sup>7,16</sup> Another characteristic feature is that once a dendritic structure is formed, it remains “frozen” and does not grow any further during subsequent increase of the applied field. Moreover, when the experiment is repeated under identical conditions, the exact field when the dendrites form and their exact patterns are never repeated. In the present films, the dendritic instability was observed only below  $T^* = 5.5$  K, whereas a

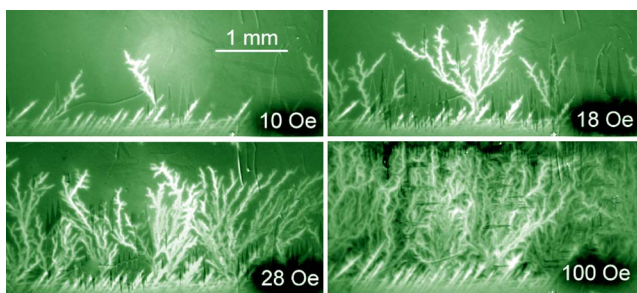


FIG. 2. (Color online) Magneto-optical images of flux distribution in a 0.29  $\mu\text{m}$  thick NbN film at 3.5 K for increasing magnetic field. The image brightness represents the magnitude of the local flux density.

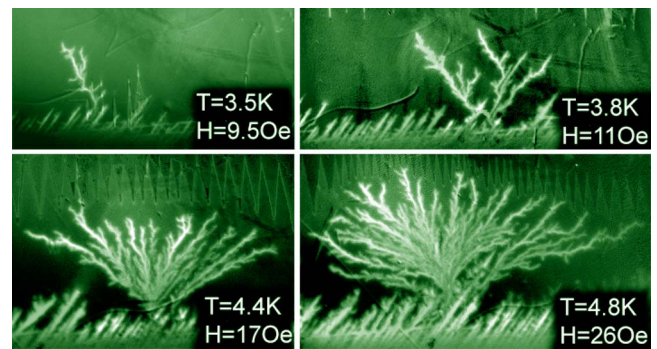


FIG. 3. (Color online) First dendrites formed in a zero-field-cooled NbN film during increasing applied field  $H$ . Dendrites formed at higher temperatures are characterized by a stronger branching.

similar threshold temperature in  $\text{MgB}_2$  is 10 K.<sup>8,11</sup> Above these threshold temperatures, the flux penetration is always spatially smooth and gradual in time.

The instability disappears not only when  $T > T^*$ , but also when the field becomes sufficiently high:  $H > H^*$  (see Fig. 1, lower panel). Our results clearly show that the threshold value depends on the field sweep direction. We propose that this dependence originates from vortex annihilation, which takes place only for the decreasing field case. Indeed, when  $H$  is increasing, the screening currents generate near the film edge a strong demagnetization field of the same sign as  $H$ . However, for decreasing  $H$ , the direction of screening currents and demagnetization field changes to the opposite. As a result, the field at the edge,  $\sim H - H_p/n$ , is expected to be negative since the demagnetization factor for the films under study is  $n \approx 10^{-3}$ , while the penetration field is  $H_p \approx 50$  Oe. This negative external field penetrates slightly inside, and there appears a line near the edge where vortices and antivortices meet.<sup>17,18</sup> Their annihilation releases additional energy that can facilitate the triggering of the instability.<sup>19</sup> Consequently, one may expect that the dendritic instability occurs in a wider range of applied fields  $H$  along the descending field branch as compared to the ascending branch.

The existence of a threshold field  $H^*$  was reported earlier in the magnetization studies of  $\text{MgB}_2$  films.<sup>20</sup> Our observed asymmetry for the increasing and decreasing field sweeps is also in agreement with results of Ref. 13, where dendritic jumps were found only for decreasing  $H$ . Interestingly, during the dendrite growth the annihilation zone may propagate very deep into the film. This is confirmed by observation of “negative” flux in the dendrite core that propagated into a film containing positive flux for a decreasing  $H$ .<sup>9</sup>

Figure 3 shows MO images of the very first dendrite formed in the 0.29  $\mu\text{m}$  thick ZFC film during four experiments at slightly different temperatures. These dendrites were formed also at different (first jump) fields  $H_{fj}$ , and there is a clear tendency that  $H_{fj}$  increases with temperature. Dendrites formed at higher  $T$  and  $H_{fj}$  are also larger in size and more branching, a tendency can be traced all the way up to  $T^* = 5.5$  K. Note also that the  $m(H)$  curve in Fig. 1 (lower panel) exhibits increasingly larger jumps as the threshold field  $H^*$  is approached. Therefore, it is a general trend that the dendritic structures have maximal size when the system is close to the stability limit; that is, for  $H \approx H^*$  or  $T \approx T^*$ .

To quantify these changes in morphology of the branching flux structures, we made a fractal analysis of their shape. The MO images were discretized to obtain a cluster of pixels

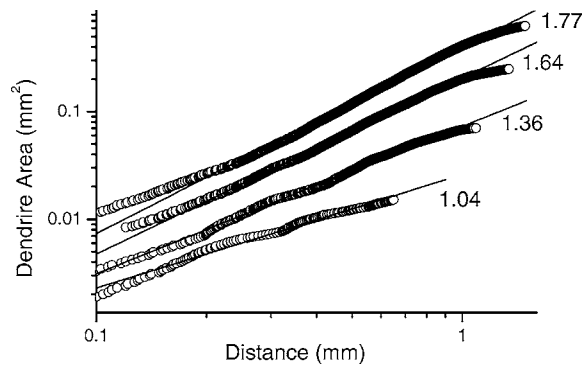


FIG. 4. Determination of fractal dimension of the first dendritic flux structure for different temperatures: 3.5, 3.8, 4.4, and 4.8 K from top to bottom. The curves are shifted vertically to avoid overlapping.

constituting a dendrite structure. A pixel belongs to the cluster if flux density averaged over its area of  $10 \times 10 \mu\text{m}^2$  exceeds some value  $H_{\min} \sim 15$  Oe. This area corresponds to four CCD pixels in the  $1280 \times 1024$  CCD array. The cluster morphology reproduced very well the apparent dendrite shape seen magneto-optically because the cores of all dendritic branches have essentially the same flux density, as discussed in Ref. 12. We calculated the number of pixels  $N(R)$  that fall inside a circle of radius  $R$  with the center at the dendrite root. The root was chosen as the pixel in the cluster that is nearest to the sample edge (linear flux structures near the edge were excluded from the analysis). If the dendritic structure is described by a power law  $N \propto R^D$ , the exponent gives the fractal dimension  $D$  of the cluster.<sup>21</sup>

The results of this analysis are presented in Fig. 4, where the actual dendrite area represents  $N$ . We find a reasonably good power-law behavior, and the fractal dimension increases with temperature (see Fig. 5 for a summary). The dimension changes from approximately unity at the lowest  $T$  to  $D=1.77$  for the most branching structure at 4.8 K. Error bars for  $D$  were found by varying  $H_{\min}$  so that the total number of pixels in the cluster changed by a factor of 2. The

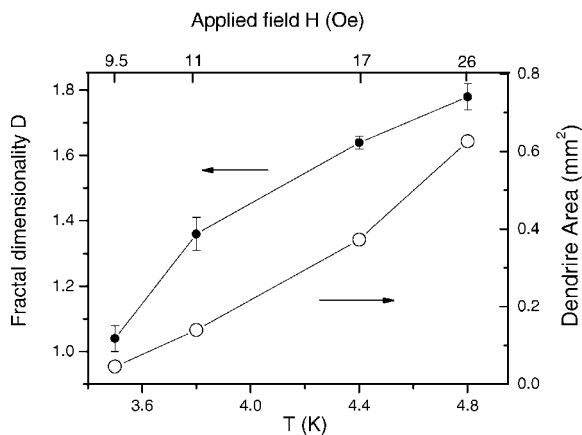


FIG. 5. Fractal dimension and total area of the first dendritic flux structure as functions of temperature or applied field.

region  $R < 0.2$  mm was ignored during the fitting since it is affected by a somewhat arbitrary choice of the circle center. Note that more branching dendrites with larger  $D$  always have a larger area.

A similar temperature dependence of dendrite morphology has been reported earlier for Nb (see Refs. 4 and 5) and for  $\text{MgB}_2$  (see Ref. 8) samples. Various degrees of branching have also been obtained by simulations taking into account the heat produced by flux motion,<sup>8,22</sup> which suggests a thermal origin of the instability. Our present results (i) give a quantitative measure of the branching ( $D$ ), (ii) show that  $D$  and dendrite area increase simultaneously, and (iii) that this increase takes place when approaching the instability threshold  $H^*(T)$  either by changing  $T$  or  $H$ .

The work was supported by the Norwegian Research Council, Grant No. 158518/431 (NANOMAT) and FUNMAT@UiO.

- <sup>1</sup>R. G. Mints and A. L. Rakhmanov, *Rev. Mod. Phys.* **53**, 551 (1981).
- <sup>2</sup>A. V. Gurevich, R. G. Mints, and A. L. Rakhmanov, *The Physics of Composite Superconductors* (Begell House, New York, 1997).
- <sup>3</sup>M. R. Wertheimer and J. de G. Gilchrist, *J. Phys. Chem. Solids* **28**, 2509 (1967).
- <sup>4</sup>C. A. Duran, P. L. Gammel, R. E. Miller, and D. J. Bishop, *Phys. Rev. B* **52**, 75 (1995).
- <sup>5</sup>M. S. Welling, R. J. Westerwaal, W. Lohstroh, and R. J. Wijngaarden, *Physica C* **411**, 11 (2004).
- <sup>6</sup>P. Leiderer, J. Boneberg, P. Brüll, V. Bujok, and S. Herminghaus, *Phys. Rev. Lett.* **71**, 2646 (1993).
- <sup>7</sup>U. Bolz, B. Biehler, D. Schmidt, B.-U. Runge, and P. Leiderer, *Europhys. Lett.* **64**, 517 (2003).
- <sup>8</sup>T. H. Johansen, M. Baziljevich, D. V. Shantsev, P. E. Goa, Y. M. Galperin, W. N. Kang, H. J. Kim, E. M. Choi, M.-S. Kim, and S. I. Lee, *Europhys. Lett.* **59**, 599 (2002).
- <sup>9</sup>T. H. Johansen, M. Baziljevich, D. V. Shantsev, P. E. Goa, Y. M. Galperin, W. N. Kang, H. J. Kim, E. M. Choi, M.-S. Kim, and S. I. Lee, *Supercond. Sci. Technol.* **14**, 726 (2001).
- <sup>10</sup>A. V. Bobyl, D. V. Shantsev, T. H. Johansen, W. N. Kang, H. J. Kim, E. M. Choi, and S. I. Lee, *Appl. Phys. Lett.* **80**, 4588 (2002).
- <sup>11</sup>Z. Ye, Q. Li, G. D. Gu, J. J. Tu, W. N. Kang, E.-M. Choi, H.-J. Kim, and S.-I. Lee, *IEEE Trans. Appl. Supercond.* **13**, 3722 (2003).
- <sup>12</sup>F. L. Barkov, D. V. Shantsev, T. H. Johansen, P. E. Goa, W. N. Kang, H. J. Kim, E. M. Choi, and S. I. Lee, *Phys. Rev. B* **67**, 064513 (2003).
- <sup>13</sup>S. C. Wimbush, B. Holzapfel, and Ch. Jooss, *J. Appl. Phys.* **96**, 3589 (2004).
- <sup>14</sup>I. A. Rudnev, S. V. Antonenko, D. V. Shantsev, T. H. Johansen, and A. E. Primenko, *Cryogenics* **43**, 663 (2003).
- <sup>15</sup>Ch. Jooss, J. Albrecht, H. Kuhn, S. Leonhardt, and H. Kronmüller, *Rep. Prog. Phys.* **65**, 651 (2002).
- <sup>16</sup>P. Leiderer (private communication).
- <sup>17</sup>E. H. Brandt and M. Indenbom, *Phys. Rev. B* **48**, 12893 (1993).
- <sup>18</sup>E. Zeldov, J. R. Clem, M. McElfresh, and M. Darwin, *Phys. Rev. B* **49**, 9802 (1994).
- <sup>19</sup>M. R. Beasley, W. A. Fietz, R. W. Rollins, J. Silcox, and W. W. Webb, *Phys. Rev.* **137**, A1205 (1965).
- <sup>20</sup>Z. W. Zhao, S. L. Li, Y. M. Ni, H. P. Yang, Z. Y. Liu, H. H. Wen, W. N. Kang, H. J. Kim, E. M. Choi, and S. I. Lee, *Phys. Rev. B* **65**, 064512 (2002).
- <sup>21</sup>J. Feder, *Fractals* (Plenum, New York, 1988).
- <sup>22</sup>I. S. Aranson, A. Gurevich, M. S. Welling, R. J. Wijngaarden, V. K. Vlasko-Vlasov, V. M. Vinokur, and U. Welp, *Phys. Rev. Lett.* **94**, 037002 (2004).